Properties of a 37 m long FRP wind turbine blade after 11 years in service

A.A. Alshannaq, J.A. Respert, L.C. Bank & T.R. Gentry
Georgia Institute of Technology, Atlanta, Georgia, USA

D.W. Scott
Georgia Southern University, Statesboro, Georgia, USA

ABSTRACT: The waste coming from decommissioned wind turbine blades poses an environmental problem since they are made primarily of Fiber Reinforced Polymers (FRPs) which are non-biodegradable materials. Millions of tons of these materials are expected to be disposed of in the coming years. Thus, responsible end-of-life (EOL) solutions are needed. The use of the blades for civil engineering infrastructure (e.g. power transmission poles, pedestrian bridge girders, highway sound barriers and roofing materials) has been proposed. In order to perform a structural and stress analysis for any of these design concepts, the as-received mechanical and physical properties of the specific type of wind blade to be used are needed. This paper presents an extensive testing program of the GFRP (Glass Fiber Reinforced Polymer) material in the spar cap of a 1.5 MW GE 37 decommissioned wind turbine blade that had been used for 11 years at a wind farm in Langford, Texas. Procedures for specimen preparation and testing are highlighted, since the blade parts have varying thicknesses (50 mm or more in some parts), layups and curvatures. As-received tensile, compressive, and shear strengths and stiffnesses were determined and compared to results from static testing of fatigued wind blades from the literature. Bolt testing was performed to obtain bearing and pull-through properties of the spar cap materials for second-life (i.e. EOL) applications where bolt performance will be a major design aspect.

1 INTRODUCTION

Fiber Reinforced Polymer (FRP) Composites have become more popular in the last few decades in the civil engineering discipline, and since then, have prompted a number of research programs due to their high strength-to-weight ratios, high stiffness-to-weight ratios, reduced weight relative to other structural materials, corrosion resistance, and durability (Bank 2006). However, some drawbacks regarding low stiffness exist, making these materials governed mostly by the serviceability limit state (SLS). Furthermore, degradation due to harsh environmental and fatigue exposures might limit their service life (Aldajah et al. 2009, Merah et al. 2010, Miller et al. 2012).

One of the major structural uses of composite materials is in the manufacturing of wind turbine blades. Relatively thick laminates used in the spar caps are bonded to a lightweight sandwich shell with sandwich composite webs as shown in Figure **1**. The advanced composite construction through vacuum-assisted resin transfer molding (VARTM) allows for highly complex geometries, lightweight construction, and substantial mechanical properties (Mishnaevsky et al. 2017). Typically, wind turbines have three wind blades (similar to airplane wings) which are connected to a rotating hub to generate electricity. However, due to uncertainty in terms of fatigue exposure, life span limits of 20-25 years are imposed on these structures, which leave these materials with significant expected structural capacity after decommissioning (Job 2013, Post et al. 2008, Lian & Yao 2010).

A sustainability problem already exists for decommissioned wind turbine blades (primarily made of Glass-FRP materials). Thousands (currently) and millions (in future years) of tons of composites now need, and will continue to need, disposal, this poses a significant threat to the environment (Liu & Barlow 2017). These materials are non-biodegradable and are currently being disposed of using landfilling and incineration. Mechanical or thermal and chemical methods are being studied for recycling. All these methods have drawbacks - in being environmentally harmful options (for the case of landfilling or incineration, which are also expected to have legislative restrictions soon) or in providing recycled fibers with reduced properties compared to composites made of virgin glass fiber (for the case of mechanical or thermal and chemical recycling of glass fiber), which eventually makes them less attractive options. Furthermore, the relative short service lives of these structures in their first life as wind

blades may allow for viable structural repurposing, defined here as using the entire wind blade or large cuts in load-bearing structural applications (e.g. bridges, poles) or consumer products (e.g. furniture, urban architecture) (Jensen & Skelton 2018).

The focus of the present work is on civil infrastructure applications, as these applications are characterized by large structures under relatively low stress levels, constructed in environments where durability and serviceability are the prominent factors in the design process.

The Re-Wind Network (www.re-wind.info) is aimed at providing greener and sustainable ways of recycling, reusing, and repurposing decommissioned wind turbine blades. The project covers various aspects regarding the end-of-life applications. The main objective of the research is to propose a methodology for dealing with end-of-life applications which will pave the way for implementation in the field by relevant stakeholders. These stakeholders could include national or local decision makers, wind turbine manufacturers and operators, or sustainable energy companies.

Extensive work is currently underway by the Re-Wind Network. The team is focused on providing various options and configurations at the small, medium, and large scale for reusing and repurposing of decommissioned wind turbine blades. A catalog published by McDonald et al. (2021) provides modeling and visualizations of different applications. Also, small and medium-scale cut parts from decommissioned wind turbine blades have been proposed by Gentry et al. (2018), Bank et al. (2018), and Gentry et al. (2020) for an affordable housing concept with design of structural and non-structural elements. Large-scale applications have been proposed by Suhail et al. (2019), and Ruane et al. (2022) as pedestrian bridge girders (the application is called BladeBridge), and by Alshannaq et al. (2021a) and Alshannaq et al. (2021b) as a power transmission pole with different voltage capacities (the application is called BladePole). To obtain key aspects and characteristics of the wind blade's geometry and properties for further analysis, work done by Tasistro-Hart et al. (2019) focused on using LiDAR scanning and point cloud data to reconstruct wind blade structures which is usually a proprietary information. The reconstruction process involved developing a software that provides 2D and 3D models to be used for further physical and mechanical analyses (the software is called BladeMachine).

All these applications will require material coupon testing to obtain strength and stiffness capacities to be checked against second-life applications and prove the efficacy of the proposal. This paper summarizes the testing of tensile, compressive, shear, bearing, and pull-through properties at the coupon-scale of the spar cap of a decommissioned 1.5 MW GE37 wind turbine blade that has a total length of 37 m and has been in service for 11 years in a wind site in Langford, Texas.

2 EXPERIMENTAL PROGRAM

Any cross-section of a wind blade consists of three major parts forming a multicellular cross-section, except the root (i.e. the end of the wind blade that connects to the hub) which is a thin-walled circular cross-section. The main structural load bearing part is the spar cap. The spar cap is mainly made of unidirectional GFRP. The aerodynamic shell is made of triaxial GFRP to resist torsional effects. The web (or webs) is principally made of biaxial GFRP to provide support to the shell and resist shear forces. Refer to Figure **1** for visualization.

2.1 *Materials*

The materials presented here are cut from the spar cap of a 1.5 MW decommissioned GE37 wind blade that has a total length of 37 m. The goal of the current research effort is to assess the as-received mechanical properties of this wind blade after 11 years in a wind farm in Langford, Texas for possible second-life applications. Spar cap samples were cut from the wind blade in the root-transition region (i.e. where the cross-section changes from circular to an aerodynamic shape) where the thickness of the material reaches 50 mm. The stacking sequence is characterized as $[(\pm45)_2/\text{Mat}/0_n/(\pm45)_2]$, where n represents a variable number of unidirectional layers (e.g. this is equal to 97 layers for one of the specimens if the assumed thickness of 0° layer is 0.4572 mm). This was obtained through burnout testing according to ASTM D2548. The average fiber mass fraction is 69% which converts to a volume fraction of 50% when a ρ_{matrix} = 1.19 g/cm^3 and ρ_{fiber} = 2.60 g/cm^3 are assumed.

The cutting of tensile, compressive, shear, bearing, and pull-through specimens involved the use of a waterjet to cut these thick composites (~50 mm). Since these materials are very thick, the cutting plan involved laying the spar cap blocks on the waterjet and cutting 6.6 mm thick strips to be easily tested for different properties. This cutting plan makes the longitudinal specimens represent the 1-3 direction rather than the 1-2 direction. However, as stated previously since the stacking sequence is mostly unidirectional, this plan is believed to provide proper approximation of the 1-2 properties, see Figure **1**. Note that since the thickness of the spar cap tapers, the width of the specimens (i.e. the total thickness of the spar cap) varies from one specimen to the other, but was approximately 50 mm.

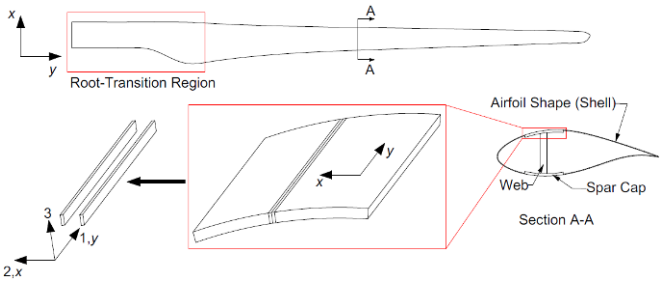

Figure 1. A sketch showing the geometry of the wind blade and the cutting plan.

2.2 *Specimens and Equipment*

The tensile testing was performed according to ASTM D3039 with specimen dimensions of 355.6 mm long × variable width × 6.6 mm thick with a gage length of 203.2 mm. The tensile modulus data were obtained through the slope of the stress-strain diagram over the 1000-3000 με range. The compressive testing was performed according to ASTM D3410 with specimen dimensions of 190.5 mm long × variable width × 6.6 mm thick with a gage length of 38.1 mm. The compressive modulus data were obtained over the same strain range (i.e. tension specimens strain range) with strain gages. Open-hole tensile testing was performed according to ASTM D5766 with specimen dimensions of 304.8 mm long × 38.1 mm width × 6.6 mm thick with a gage length of 152.4 mm and a hole diameter of 6.35 mm resulting in a width-to-diameter ratio of 6 and a diameter-to-thickness ratio of 0.96.

For the in-plane shear properties, testing was performed according to ASTM D5379 with specimen dimensions of 76.2 mm long × 11.4 mm width "measured in the notch region" × 6.6 mm thick containing only unidirectional glass fiber. The width of the specimen was 19.1 mm for the regions outside the v-notch. The shear modulus data were obtained through the slope of the stress-strain diagram over 2500-6500 με range, while the interlaminar shear properties were determined through ASTM D2344 with specimen dimensions of 38.1 mm long × 12.7 mm width × 6.6 mm thick containing only unidirectional glass fiber.

Bearing testing was performed according to ASTM D953; since the material is thick which presented difficulties testing with single or double shear fixtures. Pin-bearing specimens were 101.6 mm long × 101.6 mm wide × variable thickness with a hole diameter of 25.4+1.6 mm. Two pin diameters were used (i.e. 19.1 mm and 25.4 mm). These two bolt dimensions were selected since the research team had access to two different types of blind bolts with these dimensions. It is important to mention that blind bolt technology is intended to be used in second-life applications since these wind blades are hollow and do not have easy access to the inside cavity. The two blind bolts used were; the RS BlindNut by RS (2021) and the BlindBolt technology by BlindBolt (2021). While for pull-through testing, ASTM D7332 was used with specimen' dimensions of 139.7 mm long × 139.7 mm wide × variable thickness with a central hole diameter of 25.4+1.6 mm. The blind bolts used were 24-mm BlindBolt and 19.1-mm RS BlindNut. Note that two different thickness ranges were used; a thin material ranging from 25.4-35.6 mm coming from the spar cap between 29-32 m from the root of GE37, and a thick material ranging from 40.6-55.9 mm coming from the spar cap in the root-transition region of GE37.

For tensile, compressive, bearing, and pull-through testing, a 250-kN 810 MTS testing machine using 69 MPa hydraulic grip pressure, while for shear testing, a 100-kN 810 MTS testing machine was used. A constant crosshead displacement of 1.27 mm/min was used according to relevant ASTM standards. Epsilon Extensometer model 3542 with a gage length of 25.4 mm and Texas Measurements strain gages were used for strain measurements. A National Instruments NI cDAQ-9178 was used to acquire simultaneous load, displacement, and strain data. Note that longitudinal and transverse testing was performed for all tested properties except interlaminar shear properties for transverse specimens. Theses specimens do not satisfy the ASTM D2344 requirement of at least 10% 0° layers in the span direction.

2.3 *Results*

The results and number of specimens are summarized in Table 1. The following notes are emphasized:

- Number of specimens for longitudinal tension modulus is 52 (47 with extensometer and 5 with strain gages).
- Number of specimens for longitudinal tension strain at failure is 5 (for specimens with strain gages only).
- Number of specimens for transverse tension modulus is 12 (for specimens with extensometer only).
- Number of specimens for transverse tension strain at failure is 9 (for specimens with extensometer only).
- Number of specimens for longitudinal compression modulus and strain at failure is 5 (for specimens with strain gages only).
- Number of specimens for v-notch longitudinal shear modulus is 3 (for specimens with strain gages only).
- Unit of pull-through data is (kN).
- For transverse compression, transverse v-notch shear, longitudinal short-beam shear, bearing, and pull-through, no strain gages were used thus no modulus or strain at failure data were reported.

- For longitudinal open-hole tension, extensometer readings were affected by the first crack and the deformation of the hole, thus no strain at failure data were reported. Also, modulus values have no meaning and thus were not reported.
- For longitudinal v-notch shear, strain gages detached before complete failure and thus no strain at failure data were reported.
- *N* stands for "Number of Specimens".
- L stands for "Longitudinal".
- T stands for "Transverse".

Figure 2 through Figure 8 show the specimens in the testing machine and their modes of failure for various tests.

Table 1. Summary of results.

Property	*N*	Strength (MPa)	Modulus (GPa)	Strain at Failure (%)
Tension (L)	53	597±54.4	36.8±1.95	1.94±0.15
Tension (T)	13	33.6±3.58	10.7±0.45	0.29±0.02
Compression (L)	74	504±39.8	42.7±2.54	1.22±0.05
Compression (T)	11	114±2.05	-	-
Open-Hole (L)	11	584±29.5	-	-
Open-Hole (T)	16	22.4±2.33	-	0.24±0.02
V-Notch Shear (L)	26	60.8±2.26	4.57±0.12	-
V-Notch Shear (T)	10	27.9±2.47	-	-
Short-Beam Shear (L)	14	55.0±3.57	-	-
Bearing – 19.1 mm pin (L)	10	302±17.4	-	-
Bearing – 19.1 mm pin (T)	10	212±9.50	-	-
Bearing – 25.4 mm pin (L)	10	296±32.2	-	-
Bearing – 25.4 mm pin (T)	10	246±10.3	-	-
Pull-though – Thin BB	10	65.6±6.50	-	-
Pull-though – Thick BB	10	84.5±2.62	-	-
Pull-though – Thin RS	10	130±6.48	-	-
Pull-though – Thick RS	10	132±5.90	-	-

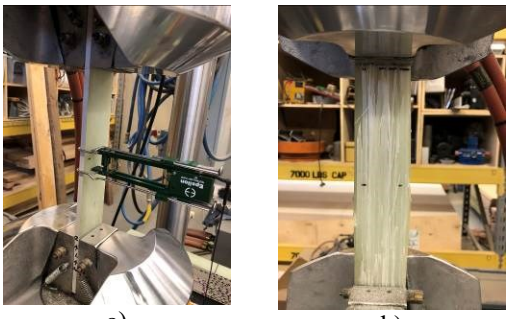

a) b)

Figure 2. Tensile specimen in the testing machine; a) with extensometer before testing, and d) after testing.

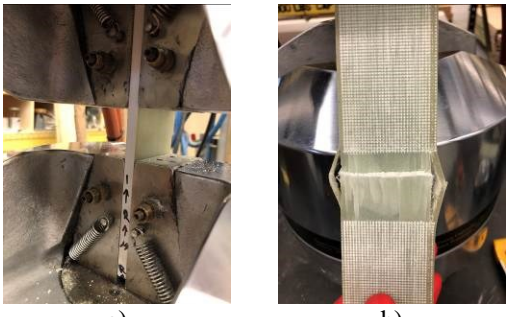

a) b)

Figure 3. Compressive specimen in the testing machine; a) before testing, and b) after testing.

a) b)

Figure 4. Open-hole tensile specimen in the testing machine; a) with extensometer before testing, and b) after testing.

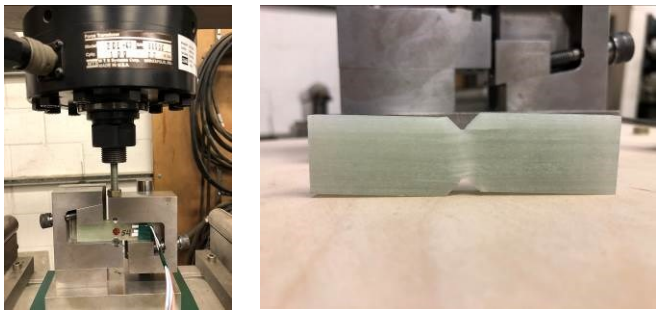

a) b)

Figure 5. V-notch shear specimen; a) in the fixture before testing, and b) after testing.

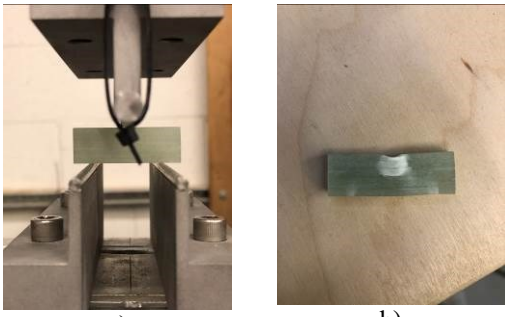

a) b)

Figure 6. Short-beam shear specimen; a) in the fixture before testing, and b) after testing.

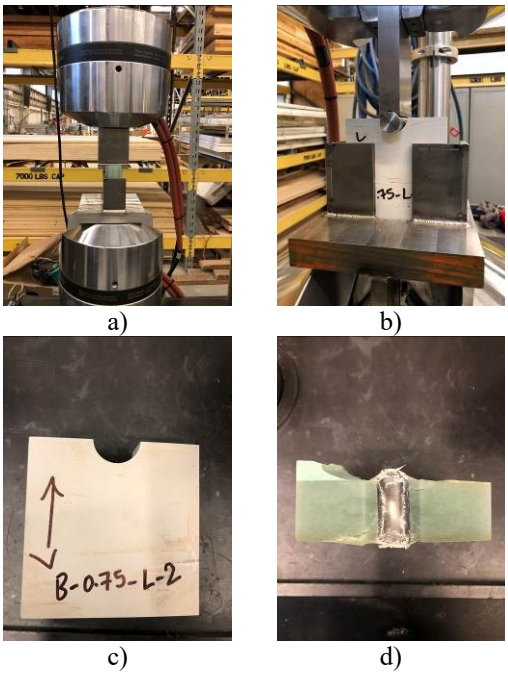

a) b)

c) d)

e)

Figure 7. Pin-bearing specimen; a-b) in the fixture before testing, c) specimen before testing, and d-e) after testing.

a)

b)

c)

d)

Figure 8. Pull-through specimen; a) in the testing fixture before testing, and b-d) after testing.

3 DISCUSSION

Table 2 shows a comparison between the obtained results and the data presented in the literature for fatigued wind blades after Sayer et al. (2013) for a 100 kW DEBRA-25 and after Ahmed et al. (2021) for a 100 kW wind blade. According to Ahmed et al. (2021), the 100-kW wind blade was made from glass fiber with a fiber weight fraction in the range of 55-60%, which is equivalent to a fiber volume fraction of 38-43%. While according to Sayer et al. (2013), the DEBRA-25 was made from glass fiber embedded in epoxy resin, however, no mass or volume fraction was reported. Note that (L) stands for "Longitudinal" and (SBS) stands for "Short-beam shear". The GE37 results provide promising strength and stiffness values for potential second-life applications by outperforming the data of 100 kW wind blades. It is important to mention that larger capacity fatigued wind blade testing (i.e. in the range of 1.0-2.0 MW) is not available in the literature, to the authors knowledge, and thus 100 kW wind blade's data are presented for comparison purposes. Also, blades that have experienced a larger number of fatigue cycles (i.e. beyond 11 years) still need testing to make proper conclusions about strength and stiffness retention.

Table 2. Comparison of test results to data from the literature.

Property	Spar Cap of GE37	Sayer et al. (2013)	Ahmed et al. (2021)
Tensile Strength - L (MPa)	597	477	350
Compressive Strength - L (MPa)	504	447	225
Shear Strength - SBS (MPa)	55.0	32.3	-
Tensile Modulus - L (GPa)	36.8	26.7	15.6
Compressive Modulus - L (GPa)	42.7	26.2	-

4 CONCLUSIONS

This paper presents results of tests of the GFRP material spar cap of a 1.5 MW decommissioned GE37 wind turbine blade for tensile, compressive, shear, bearing, and pull-through properties. The following conclusions can be drawn from the results:

- Strength and stiffness properties of the GE37 after 11 years in a wind farm provide values which outperform the data published previously on 100 kW fatigued wind blades. More testing with age and capacity is still needed to judge strength and stiffness retention levels.
- Data presented herein can be used for structural analysis and design, and pave the way toward reliability-based strength reduction factors for second-life applications of decommissioned wind turbine blades.
- Bolts through the thick spar cap of a 1.5 MW GE37 wind blade for second-life applications can achieve full-capacity of the bolt itself when blind bolting techniques (i.e. RS BlindNut and BlindBolt) are employed.

5 ACKNOWLEDGEMENTS

Support for this research was provided by the National Science Foundation (NSF) under grants 2016409, 1701413, and 1701694; by InvestNI/Department for the Economy (DfE) under grant 16/US/3334 and by Science Foundation Ireland (SFI) under grant USI-116 as part of the US-Ireland Tripartite research program.

The authors would like to thank Logisticus Group for supplying the spar cap specimens for testing and would like to thank the Wisconsin Structures and Materials Laboratory at University of Wisconsin-Madison for loaning the Iosipescu fixture for shear v-notch testing.

6 REFERENCES

Ahmed, M. M. Z., Alzahrani, B., Jouini, N., Hessien, M. M. & Ataya, S. 2021. The Role of Orientation and Temperature on the Mechanical Properties of a 20 Years Old Wind Turbine Blade GFR Composite. *Polymers,* 13: 1144.

Aldajah, S., Alawsi, G. & Rahmaan, S. A. 2009. Impact of Sea and Tap Water Exposure on the Durability of GFRP Laminates. *Materials and Design,* 30: 1835-1840.

Alshannaq, A. A., Bank, L. C., Scott, D. W. & Gentry, R. 2021a. A Decommissioned Wind Blade as a Second-Life Construction Material for a Transmission Pole. *Construction Materials,* 1: 95-104.

Alshannaq, A. A., Bank, L. C., Scott, D. W. & Gentry, T. R. 2021b. Structural Analysis of a Wind Turbine Blade Repurposed as an Electrical Transmission Pole. *Journal of Composites for Construction,* 25: 04021023.

ASTM-D953 2019. Standard Test Method for Pin-Bearing Strength of Plastics. West Conshohocken, PA: ASTM International.

ASTM-D2344 2016. Standard Test Method for Short-Beam Strength of Polymer Matrix Composite Materials and Their Laminates. West Conshohocken, PA: ASTM International.

ASTM-D2584 2018. Standard Test Method for Ignition Loss of Cured Reinforced Resins. West Conshohocken, PA: ASTM International.

ASTM-D3039 2017. Standard Test Method for Tensile Properties of Polymer Matrix Composite Materials. West Conshohocken, PA: ASTM International.

ASTM-D3410 2016. Standard Test Method for Compressive Properties of Polymer Matrix Composite Materials with Unsupported Gage Section by Shear Loading. West Conshohocken, PA: ASTM International.

ASTM-D5379 2019. Standard Test Method for Shear Properties of Composite Materials by the V-Notched Beam Method. West Conshohocken, PA: ASTM International.

ASTM-D5766 2018. Standard Test Method for Open-Hole Tensile Strength of Polymer Matrix Composite Laminates. West Conshohocken, PA: ASTM International.

ASTM-D7332 2016. Standard Test Method for Measuring the Fastener Pull-Through Resistance of a Fiber-Reinforced Polymer Matrix Composite. West Conshohocken, PA: ASTM International.

Bank, L. C. 2006. *Composites for Construction: Structural Design with FRP Materials,* Hoboken, NJ: Wiley.

Bank, L. C., Arias, F. R., Yazdanbakhsh, A., Gentry, T. R., Al-Haddad, T., Chen, J.-F. & Morrow, R. 2018. Concepts for Reusing Composite Materials from Decommissioned Wind Turbine Blades in Affordable Housing. *Recycling,* 3: 11.

BlindBolt. 2021. *Blind-Bolt Technology* [Online]. Available: https://www.blindbolt.co.uk/the-blind-bolt/technical-data/ [Accessed April 22, 2021].

Gentry, R., Bank, L. C., Chen, J. F., Arias, F. & Al-Haddad, T. Adaptive Reuse of FRP Composite Wind Turbine Blades for Civil Infrastructure Construction. In Benzarti, K., Quiertant, M., Ferrier, E. & Caron, J. F., (eds.) *Proceedings of the 9th International Conference on Fiber-Reinforced Polymer Composites in Civil Engineering (CICE 2018), Paris, France, July 17-19, 2018*. Paris, France: IIFC, 692-698.

Gentry, T. R., Al-Haddad, T., Bank, L. C., Arias, F. R., Nagle, A. & Leahy, P. 2020. Structural Analysis of a Roof Extracted from a Wind Turbine Blade. *Journal of Architectural Engineering,* 26: 04020040.

Jensen, J. P. & Skelton, K. 2018. Wind Turbine Blade Recycling: Experiences, Challenges and Possibilities in a Circular Economy. *Renewable and Sustainable Energy Reviews,* 97: 165-176.

Job, S. 2013. Recycling Glass Fibre Reinforced Composites – History and Progress. *Reinforced Plastics,* 57: 19-23.

Lian, W. & Yao, W. 2010. Fatigue Life Prediction of Composite Laminates by FEA Simulation Method. *International Journal of Fatigue,* 32: 123-133.

Liu, P. & Barlow, C. Y. 2017. Wind Turbine Blade Waste in 2050. *Waste Management,* 62: 229-240.

McDonald, A., Kiernicki, C., Bermek, M., Zhang, Z., Poff, A., Kakkad, S., Lau, E., Arias, F., Gentry, R. & Bank, L. 2021. *Re-Wind Design Catalog Fall 2021* [Online]. Available: https://static1.squarespace.com/static/5b324c409772ae52fecb6698/t/618e5b5f5c9d244eec10e788/1636719473969/Re-Wind+Design+Catalogue+Fall+2021+Nov+12+2021+reduced+size.pdf [Accessed December 20, 2021].

Merah, N., Nizamuddin, S., Khan, Z., Al-Sulaiman, F. & Mehdi, M. 2010. Effects of Harsh Weather and Seawater on Glass Fiber Reinforced Epoxy Composite. *Journal of Reinforced Plastics and Composites,* 29: 3104-3110.

Miller, D., Mandell, J., Samborsky, D., Hernandez-Sanchez, B. & Griffith, D. T. 2012. Performance of Composite Materials Subjected to Salt Water Environments. *53rd AIAA/ASME/ASCE/AHS/ASC Structures, Structural Dynamics and Materials Conference.* Honolulu, Hawaii.

Mishnaevsky, L., Branner, K., Petersen, H. N., Beauson, J., McGugan, M. & Sørensen, B. F. 2017. Materials for Wind Turbine Blades: An Overview. *Materials,* 10: 1285.

Post, N. L., Case, S. W. & Lesko, J. J. 2008. Modeling the Variable Amplitude Fatigue of Composite Materials: A Review and Evaluation of the State of the Art for Spectrum Loading. *International Journal of Fatigue,* 30: 2064-2086.

RS. 2021. *RS Pole Blind Nut Technology* [Online]. Available: https://www.rspoles.com/sites/default/files/resources/RS%20Poles%20Metric%20Installation%20Guide%20V2.2c.pdf [Accessed April 22, 2021].

Ruane, K., Zhang, Z., Nagle, A., Huynh, A., Alshannaq, A., McDonald, A., Soutsos, M., Niblock, C., McKinley, J. & Leahy, P. Experimental Investigation of an FRP Wind Turbine Blade for use as a Bridge Girder. *2022 TRB Annual Meeting, Washington DC, USA, January 9-13, 2022*.

Sayer, F., Bürkner, F., Buchholz, B., Strobel, M., van Wingerde, A. M., Busmann, H.-G. & Seifert, H. 2013. Influence of a Wind Turbine Service Life on the Mechanical Properties of the Material and the Blade. *Wind Energy,* 16: 163-174.

Suhail, R., Chen, J.-F., Gentry, T. R., Tasistro-Hart, B., Xue, Y. & Bank, L. C. Analysis and Design of a Pedestrian Bridge with Decommissioned FRP Windblades and Concrete. *Proceedings of the 14th International Symposium on Fiber-Reinforced Polymer Reinforcement of Concrete Structures (FRPRCS), Belfast, UK, June 4-7, 2019*. Belfast, UK: IIFC, 1-5.

Tasistro-Hart, B., Al-Haddad, T., Bank, L. C. & Gentry, R. Reconstruction of Wind Turbine Blade Geometry and Internal Structure from Point Cloud Data. *Proceedings of the 2019 ASCE International Conference on Computing in Civil Engineering (i3CE 2019), Atlanta, Georgia, June 17-19, 2019*. American Society of Civil Engineers, 130-137.